STOL Potential of the Circulation Control Wing for High-Performance Aircraft

Robert J. Englar,* Lynn A. Trobaugh,† and Rodney A. Hemmerly‡
David W. Taylor Naval Ship Research and Development Center, Bethesda, Md.

Research and development being conducted at the David Taylor Naval Ship R and D Center investigates the STOL capability of the Circulation Control Wing (CCW) concept on high-performance aircraft. This high-lift system, which employs tangential blowing over a rounded trailing edge and requires mass flows characteristic of state-of-the-art turbine engine bleed, has demonstrated the ability to more than double the lift capability of conventional Navy and Marine aircraft. The resulting reduced takeoff and landing speeds and distances, plus increased overload capability, are achieved without severe compromise of wing structure, weight, or engine arrangement, and without large quantities of ducted hot gas. Based on these anticipated benefits and the results of existing experimental investigations, a program has been initiated to demonstrate the STOL capability of the CCW concept applied to a full-scale A-6 flight demonstrator aircraft. This paper will address the experimental development and optimization of the CCW system on an A-6 model and will present predicted full-scale STOL performance gains for the flight demonstrator.

Introduction

WITH the current renewal of interest in STOL and V/STOL aerodynamics, a number of powered lift concepts are undergoing development in an attempt to derive maximum lifting benefits from various combinations of advanced lifting surfaces augmented by engine thrust or bleed. Whereas quite large net lift can be generated by many of these designs, a number of compromises are required for actual implementation on high-performance aircraft. Rather severe impact is felt on wing complexity and structural design of augmentor and ejector wing aircraft, while engine placement and nacelle design required for upper surface blowing and externally blown flap concepts are often not compatible with high-performance fighter and attack configurations. A more feasible concept for these aircraft is a high-lift system which can be easily incorporated into conventional wing trailing edge structure, and can be powered by bleed air from existing turbine engines without major modifications or relocation. Technology[1] developed at the David Taylor Naval Ship R&D Center (DTNSRDC) since 1968 has led to the Circulation Control Wing (CCW), a STOL concept offering this potential.

The basic aerodynamics of the circulation control concept involve the adherence of a thin, tangentially ejected jet sheet to the rounded trailing edge of an otherwise conventional airfoil. This phenomenon, frequently identified as the Coanda effect, is produced by a balance within the jet sheet between centrifugal force and the low static pressure produced by the jet velocity (Fig. 1). This device initially acts as a boundary-layer control, but achieves its high-lift capability by control of the airfoil stagnation points and thus the circulation around it. Due to the lack of a sharp trailing edge and the associated Kutta condition, this circulation control is achieved at considerably lower momentum coefficients than the somewhat similar tangentially blown flap.[2-4]

Presented as Paper 77-578 at the AIAA/NASA Ames V/STOL Conference, Palo Alto, Calif., June 6-8, 1977; submitted Sept. 19, 1977; revision received Dec. 8, 1977.

Index categories: Aerodynamics; Performance; Jets, Wakes, and Viscid-Inviscid Flow Interactions.

*A-6/CCW Program Manager and Sr. Aerospace Engineer. Member AIAA.

†Sr. Aerospace Engineer, Aircraft Division.

‡Aerospace Engineer, Aircraft Division.

The primary mechanism of the CCW lift augmentation is the increased streamline deflection which accompanies movement of the stagnation points; the overall result is to produce an effective camber considerably greater than the geometric value. Whereas the CCW does not generate the same ultrahigh lift coefficient (much of which is vertical thrust component) achieved by the externally blown flap and upper surface blowing concepts, it appears to be a very promising concept for high-performance attack and fighter aircraft, where engine placement below or on the wing is not practical and where available C_μ may be low.

Exploratory investigations of the concept applied to conventional airfoils and wings have demonstrated a threefold gain in lift over the conventional flapped airfoil section,[2,3] and at least a doubling of maximum C_L for a three-dimensional (3-D) aircraft configuration.[5,6] These results were sufficient to cause initiation of a flight test program to verify the CCW concept on an operational test bed aircraft. The goals of the program are to demonstrate maximum obtainable lift augmentation from the CCW powered by engine bleed air; to evaluate stability, control, and handling characteristics in the STOL regime; and to develop the technology to the point of reducing the risk of application to future STOL designs. The Grumman A-6 was chosen as the test bed demonstrator aircraft because of its excellent aerodynamic configuration (high aspect ratio, flap span, and tail volume coefficient; moderate sweep and airfoil thickness), availability of a test aircraft, relative simplicity of trailing edge modifications, twin engines with additional bleed ports available, and predicted STOL performance gains with CCW. A wind-tunnel experimental program was conducted to

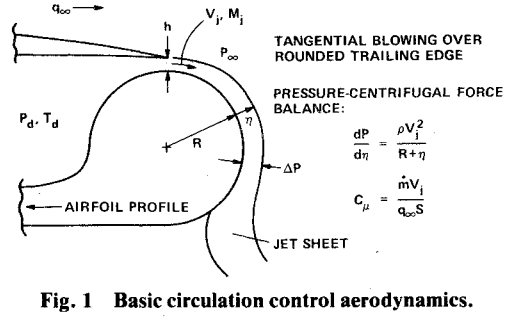

Fig. 1 Basic circulation control aerodynamics.

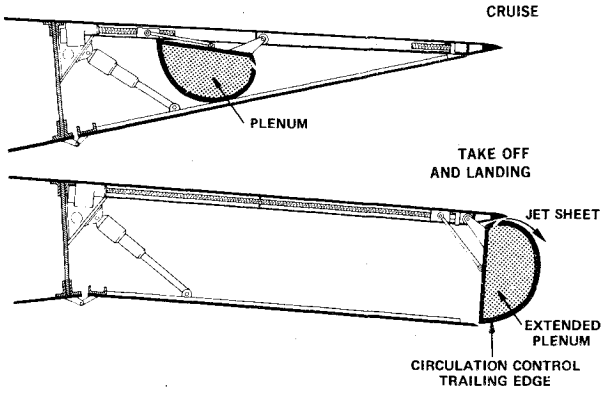

Fig. 2 Extended trailing-edge CCW configuration.

optimize the lifting surface configuration and provide the data base for the flight test. The following sections will describe the details and results of these investigations.

Two-Dimensional Airfoil Evaluation

A two-dimensional model of the A-6 wing fold-line airfoil section (NACA 64A008.4 modified) was constructed for evaluation in a 3×8-ft 2-D test section inserted in the DTN-SRDC 8×10-ft south subsonic wind tunnel. Of the several possible means of converting a cruise airfoil into the CCW configuration,[2] the trailing edge was modeled to resemble the extended configuration shown in Fig. 2, as this appeared most feasible for the flight demonstrator modification. Details of the model are shown in Fig. 3. Data acquisition was by static pressure integration over the model and a wake rake downstream; test technique was very similar to that used in Refs. 3 and 7. Variations in slat gap, slat angle, jet slot height, trailing edge shape, airfoil incidence, and momentum coefficient were investigated in order to optimize the leading- and trailing-edge parameters for maximum lift augmentation. Airfoil lift, as a function of blowing and incidence, is plotted in Fig. 4. Lift coefficients of almost 6.5 generated by the airfoil with a 37.5 deg slat deflection were limited at higher incidence by upper surface flow separation from the slat leading edge. Whereas this was controlled somewhat by additional slat deflection, net lift was not greatly improved by this means, due to reduction in the vertical force component on the slat as it was tilted forward. An increase in the radius at the sharp edge of the main airfoil exposed at the slat gap (Fig. 3) proved quite effective, and seemed promising for application on the slat as well. However, this improved slat was not tested on the 2-D model, as the preceding results were sufficiently high to warrant modification of a 1/8.5-scale A-6 model with the trailing-edge parameters of the 2-D section and provision for additional leading-edge investigation.

Three-Dimensional A-6/CCW Investigations

Model

A 1/8.5-scale model of the A-6A obtained from Grumman Aerospace Corporation was modified to the CCW configuration, as shown in Fig. 5. The conventional flap was removed and replaced with the rounded trailing edge developed in the 2-D test, Fig. 3, with parameters h/R, R/C, and h/C constant across the span. Flow fences, to prevent spanwise flow from unblown areas, were added at inboard and outboard flap stations. Figure 6 depicts these modifications to the wing trailing edge and shows, by means of a cotton tuft, the 180 deg or more of jet turning produced statically by the Coanda effect. The wing plenums could be controlled independently to balance the flows or provide differential blowing between the wings for roll control. Jet slot height h was also adjustable to balance the flow and investigate the effect of variation in parameters h/R and h/C. Provisions were made to allow variation of slat angle and gap and leading edge radius. Spoilers, horizontal stabilizer, and rudder could be deflected to or beyond the deflection ranges on the full-scale aircraft. Engine inlets and exhausts were faired in with streamlined contours to avoid the complexity of flow-through testing. Jet mass flow $\dot{m}$ was measured by venturimeter in the air supply line, and jet velocity was calculated assuming isentropic expansion from duct total pressure at the wing plenum midspan, P_d, to freestream static pressure

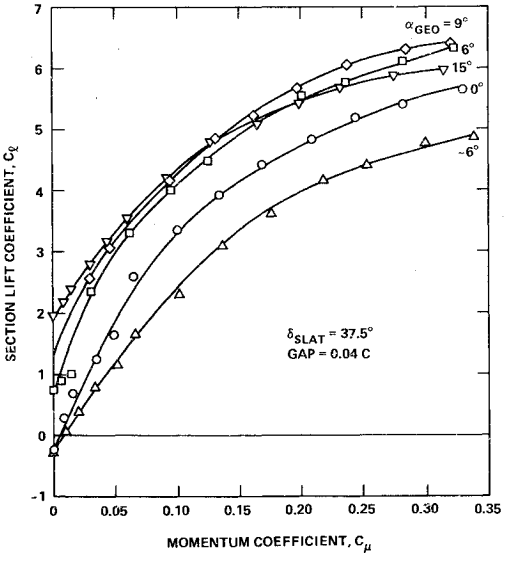

Fig. 4 Two-dimensional lift characteristics of the 64A008.4/CCW airfoil.

$$V_j^2 = \frac{2\gamma R' T_d}{\gamma - 1}\left[1 - \left(\frac{P_\infty}{P_d}\right)^{(\gamma-1)/\gamma}\right] \quad (1)$$

where R' is the universal gas constant, 1715 $ft^2/s^2{}^\circ R$. The momentum coefficient was then calculated as

$$C_\mu = \dot{m} V_j / q_\infty S \quad (2)$$

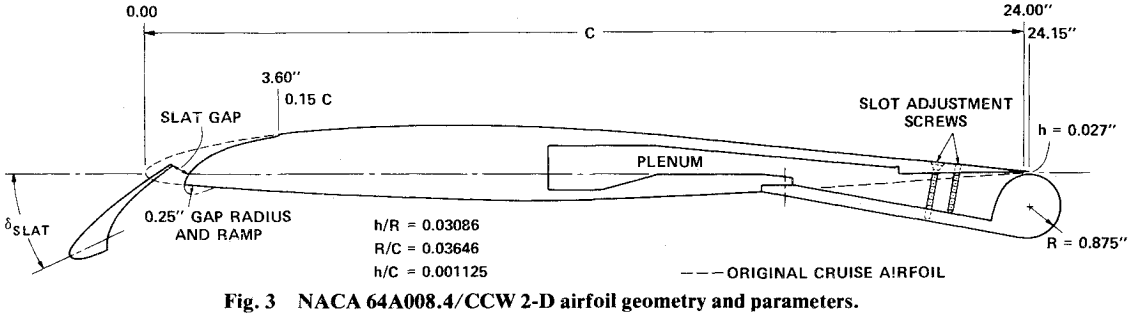

Fig. 3 NACA 64A008.4/CCW 2-D airfoil geometry and parameters.

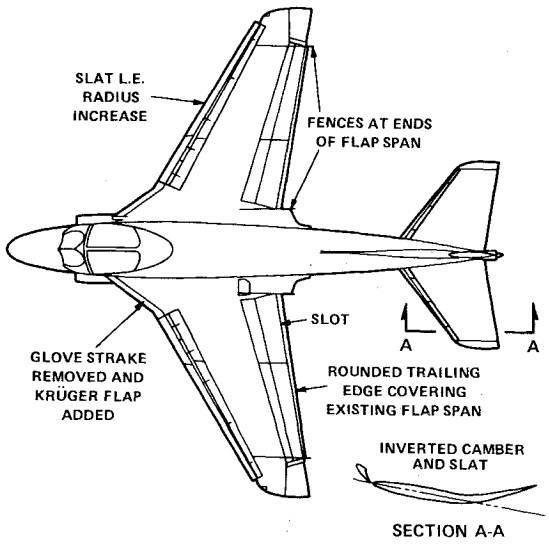

Fig. 5 A-6/CCW wing and tail modifications.

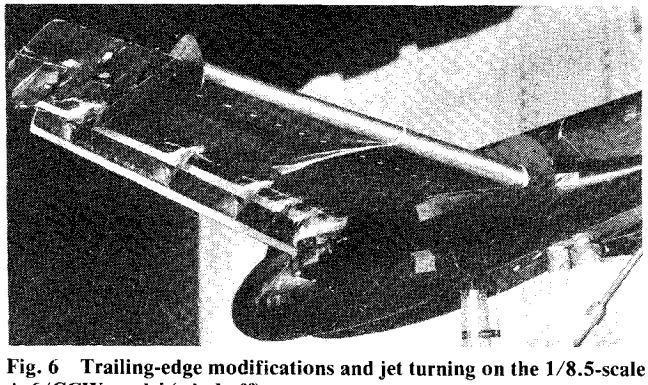

Fig. 6 Trailing-edge modifications and jet turning on the 1/8.5-scale A-6/CCW model (wind off).

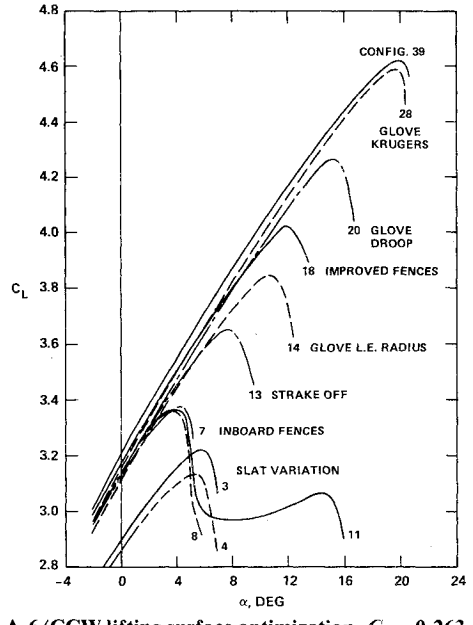

Fig. 7 A-6/CCW lifting surface optimization, $C_\mu = 0.263$, tail off.

Lifting Surface Optimization

Over 600 hours of wind-tunnel investigations were run to optimize the A-6/CCW lifting surface, to determine trimmed force coefficients, to verify longitudinal and directional stability and control characteristics and performance in ground effect, and to generate other supporting data to assure flight safety of the modified aircraft. From the early stages of the lifting surface portion of the test, it was apparent that some type of leading-edge problem was producing stall-inducing flow separation at incidences above 4 to 6 deg (Fig. 7 and Ref. 9). Variations in slat deflection, gap, or leading edge radius (Configurations 3, 4, 7, 8, and 11) did not improve this condition. Tuft studies showed that the leading-edge glove located at the wing/body junction was the source of a strong vortex and separated flow region which swept back to the trailing edge in the vicinity of the inboard slot end. Additional flow disturbance began at the outboard edge of the slat and was strongly influenced by the vortex from the glove. Removal of a sharp leading-edge strake on the glove showed significant improvement (Configuration 13), and rounding or deflection of the glove leading edge (Configurations 14, 20, 28, and 39) showed continued elimination of separation and vorticity. Including some changes in flow fences and slat gap, Fig. 7 shows that, for a constant $C_\mu = 0.263$ and no changes in trailing edge parameters, improvement in the leading-edge and glove geometry increased $C_{L_{max}}$ from 3.1 to 4.6 and stall angle from 4 to 20 deg. Figure 8 presents variations in the tail-off lift, drag, and pitching moment curves with blowing for the optimized wing (Configuration 39), and a comparison to the conventional A-6 high-lift system (semi-Fowler flap with 30 deg deflection, and 15% chord slat with 25 deg deflection and 2% gap) tested on the same model.[8] With the optimized wing, $C_{L_{max}}$ can be increased by a factor of 2.2 at $C_\mu = 0.30$.

Tail Development and Longitudinal Trim

The rather large nose-down pitching moments associated with blown systems of this type are evident in Fig. 8, and suggest that the existing all-moving horizontal stabilizer will require some improvement in order to assure longitudinal trim. It was also suspected that the large streamline curvature produced by the blowing would generate large downwash angles and significant reduction in dynamic pressure at the tail plane. To investigate this, downwash angles were measured from photographs of cotton tufts attached to wires strung vertically from tunnel floor to ceiling at several spanwise locations along the tail quarter-chord position (the horizontal tail surfaces were removed). Downward tuft deflections as high as 38 deg from the horizontal at the tailtip plane were observed.[9] Because the outer portions of the tail were immersed in the strong wingtip vortex, large variations in ϵ were found along the span, and locations near the tip were expected to experience rather serious stall. In addition, measurement[9] of the dynamic pressure at the tail mean aerodynamic chord location showed as much as 45% loss from the freestream value, but losses of only 10% or less at a location atop the vertical tail.

Both the dynamic pressure and the downwash measurements pointed to a high T-tail for trim, a frequent solution on many STOL designs encountering similar problems. However, that configuration was not practical for this program due to cost considerations for the full-scale modification, and thus a program of improving the existing all-moving stabilizer was undertaken. Figure 9 depicts sample results of these investigations for a stabilizer setting of -18 deg and $C_\mu = 0.10$. The conventional tail (Configuration 46) is unable to trim the nose-down moment shown in Fig. 8, and suffers a severe leading-edge stall through much of the aircraft incidence range due to the large downwash angles. Addition of a 17% chord elevator deflected -20 deg (trailing edge upward) increased tail inverted camber (Configuration 52), resulting in a substantial nose-up moment and reduced leading-edge separation. Further increase in elevator length or deflection (Configurations 61-63) provided additional tail download and nose-up moment. Structural considerations on the full-scale modification and the need for additional tail download at higher C_μ led to Configuration 122, the cambered stabilizer shown in Fig. 5. Here, the conventional

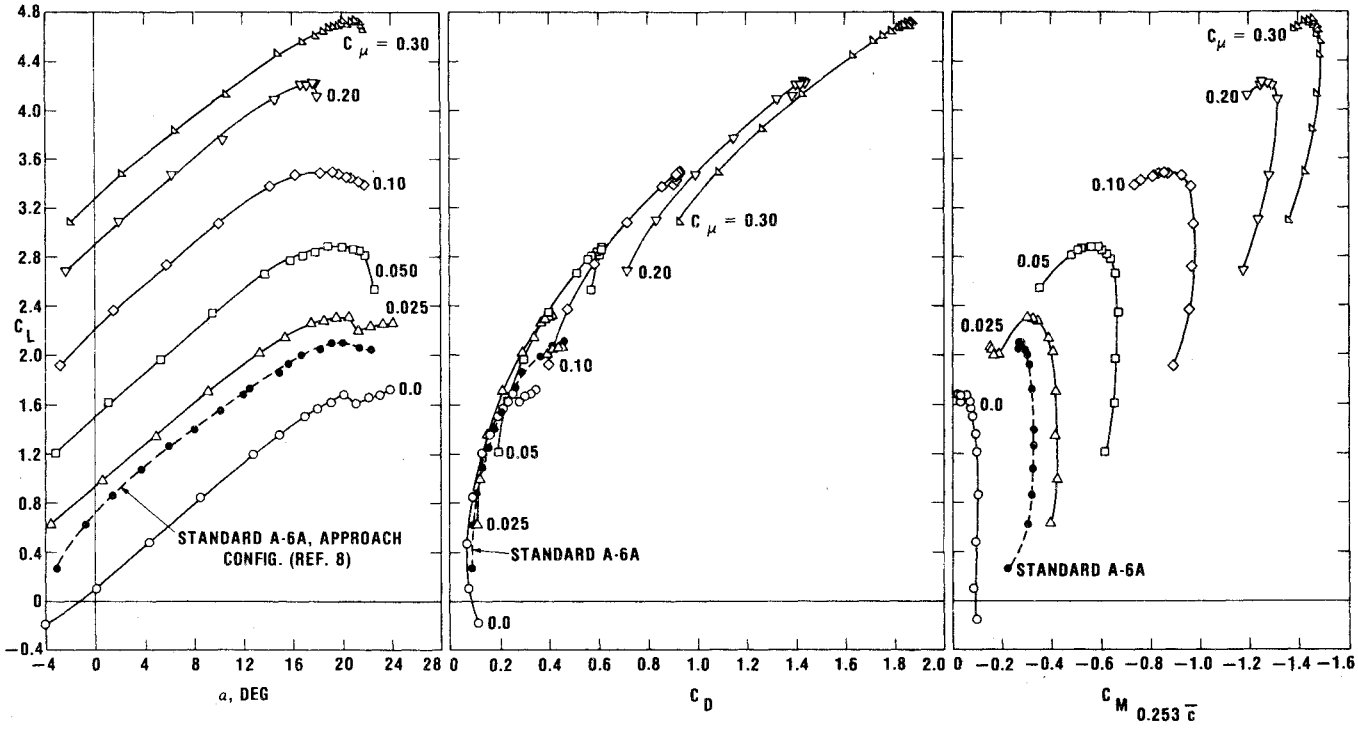

Fig. 8 Optimized A-6/CCW tail-off lift, drag, and pitching moment.

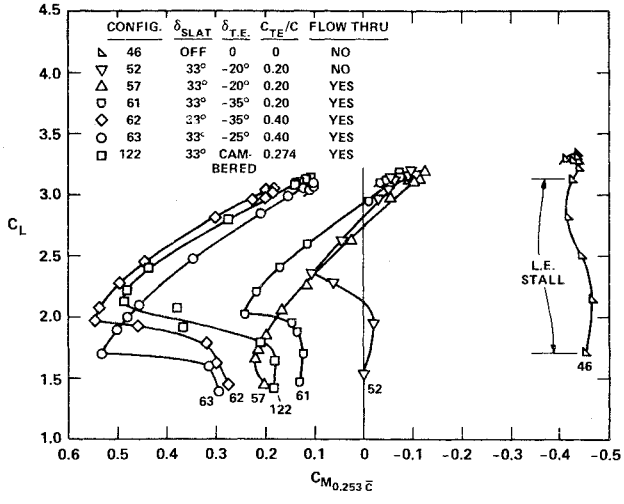

Fig. 9 Horizontal tail development, $C_\mu = 0.10$, $i_S = -18$ deg.

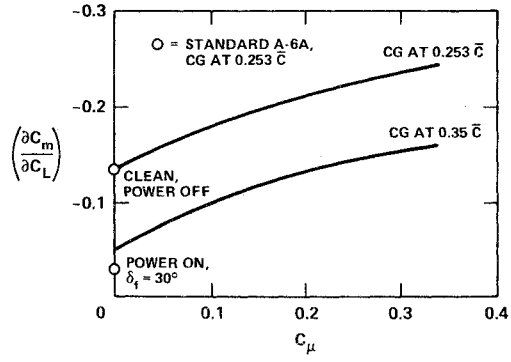

Fig. 10 A-6/CCW stability levels vs C_μ (tail on).

stabilizer aft of the 60% chord and the elevator previously mentioned were replaced with a smoothly curved and cambered trailing edge which extended the projected chord by 27.4%. Although outboard stall still exists at lower C_L, indications are that modification of the strong vortex located at the wing/body juncture can reduce the downwash. Removal of the streamlined inlet and exhaust fairings (Configuration 57) allowed freestream dynamic pressure to flow through the model and exit at the engine exhaust nozzle into the core of the vortex. Elimination of tail stall between Configurations 52 and 57 in Fig. 9 implies that a similar favorable effect will probably result from jet engine exhaust on the full-scale flight demonstrator.

The trim problem at higher C_μ can be further reduced by pitching moment resolution about further aft center-of-gravity (c.g.) locations. The excellent longitudinal stability levels of the CCW configuration are shown in comparison to the conventional A-6 in Fig. 10. Here the increased tail size and aft center-of-pressure due to blowing combine to produce stability levels ($\partial C_m/\partial C_L$) at $0.25\bar{C}$, considerably higher than the A-6 in conventional approach configuration. This allows aft c.g. shift of 10% or more and provides trim up to $C_\mu = 0.30$ with the existing tail maximum deflection of -24 deg. Thus, no tail control rerigging is required by the blowing, and the flight demonstrator with c.g. at $0.35\bar{C}$ will still be more longitudinally stable than the conventional A-6 with 30 deg flap deflection.

Trimmed Data

Variation in stabilizer incidence for the cambered tail (Configuration 122) was conducted at each of five blowing coefficients to generate the trim lift and drag data of Figs. 11 and 12. In these data, landing gear are down, the engine inlets are flow-through, and the wing slat has been set to 25 deg to match the existing deflection on the actual aircraft. Flow attachment, which had been provided by the 37.5 deg slat deflection of Configuration 39, is retained by an increase in leading edge radius on the 25 deg slat. Trim $C_{L_{max}}$ is 2.1 times that for the conventional A-6 (although its c.g. is at the quarter-chord in the data of Ref. 8). The unblown data ($C_\mu = 0$) for the modified configuration shows a somewhat greater $C_{L_{max}}$ than the conventional aircraft, indicating that, in the event of a blowing failure, the CCW configuration would retain landing characteristics similar to the con-

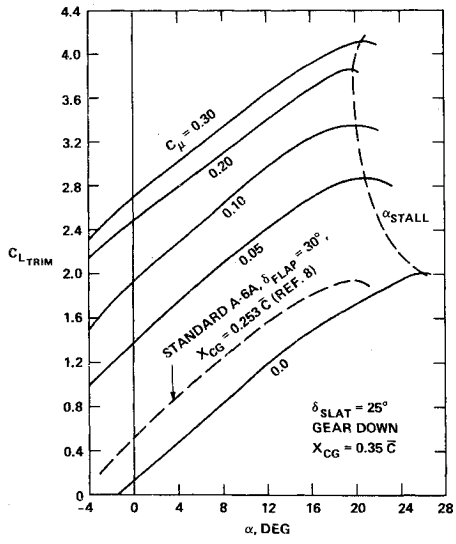

Fig. 11 Trimmed lift data for the optimized A-6/CCW configuration.

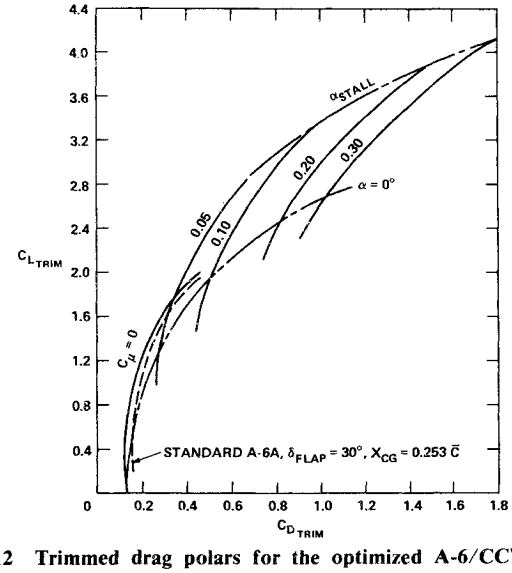

Fig. 12 Trimmed drag polars for the optimized A-6/CCW configuration.

ventional A-6. Trimmed drag polars, significantly higher than the conventional, can offset engine thrust and allow approaches at higher power settings, thus reducing time for engine spin-up in the event of a wave-off. Unlike many of the blown high-lift concepts, no thrust component results from increased momentum efflux; the aircraft can thus be stabilized in equilibrium flight down steep glide slopes at reduced approach speeds, as thrust is balanced by induced drag. For this configuration, largest gains in lift augmentation and associated induced drag are for momentum coefficients of less than 0.15. It is interesting to note that at zero incidence, $C_L = 2.7$ can be achieved for $C_\mu = 0.30$ compared to $C_L = 0.5$ for the conventional A-6; approach at greatly reduced incidence and improved pilot visibility is thus a strong possibility.

Additional Supporting Data

A significant amount of additional data was generated to verify the longitudinal and directional stability and control characteristics and handling qualities of the A-6/CCW. Included were the investigation of roll control by use of both spoilers and differential blowing, as well as poststall and stall hysteresis studies, all of which are presented in Ref. 9. These data were provided to Grumman Aerospace Corporation,

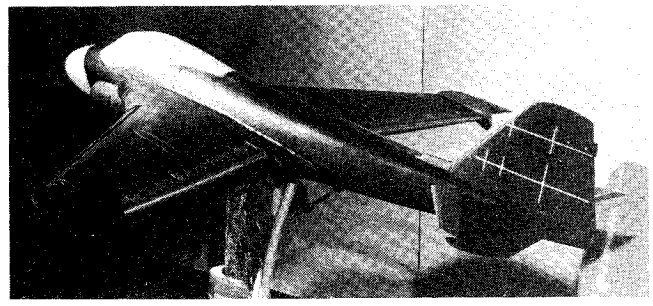

Fig. 13 1/8.5-scale model of the A-6/CCW flight test configuration.

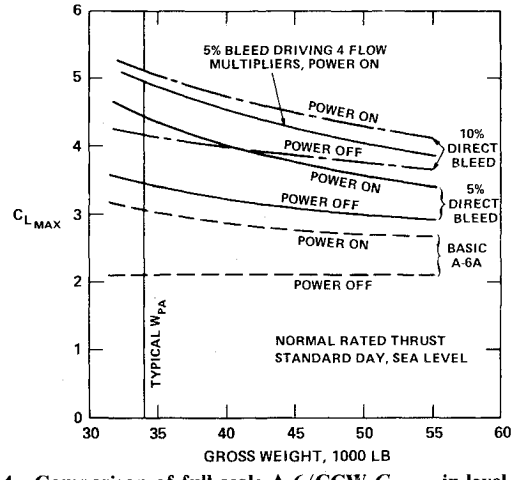

Fig. 14 Comparison of full-scale A-6/CCW $C_{L_{max}}$ in level flight at normal rated thrust.

which was awarded a contract to conduct an eight-month feasioility study of modifying an A-6A with a circulation control wing. The study concluded that the flying qualities of the modified test-bed vehicle are expected to be adequate for pilot demonstration of the aircraft, and that no major flight control system changes are necessary.

Flight Test Configuration

It was realized that several changes to the preceding model configuration should be made and evaluated, both to simplify aircraft modifications and to improve on the performance indicated by the preceding data. To simplify the wing, the inboard flow fence and an enlarged radius on the wing leading edge exposed behind the slat gap were removed, and the jet slot height was reduced from $h/R = 0.0309$ to 0.0231. The net lift change was slight, being negligible at no blowing, and varying almost linearly to $\Delta C_L = -0.17$ at $C_\mu = 0.30$. The cambered horizontal stabilizer was found to generate too much download, making trim at $C_\mu = 0$ impossible without rerigging the stabilizer control to add about 10 deg of additional nose-up incidence. At this incidence, the inverted slat would be inclined upward about 46 deg from the fuselage reference line, and flow separation was a certainty. To eliminate these problems, the slat was replaced by an inverted droop at a lesser deflection, and its leading-edge radius was increased. Also, the cambered aft section was replaced with the conventional trailing edge plus a 40% chord extension fixed at -10 deg deflection. The reconfigured model is shown in Fig. 13. The net changes in trimmed $C_{L_{max}}$ with this final configuration were found to be -0.09, -0.07, and -0.14 relative to Fig. 11 for $C_\mu = 0$, 0.10, and 0.30, respectively.

STOL Performance Predictions

The model investigations thus confirmed that significant high-lift potential was provided by the concept and that sufficient trim and control power were available with the A-6

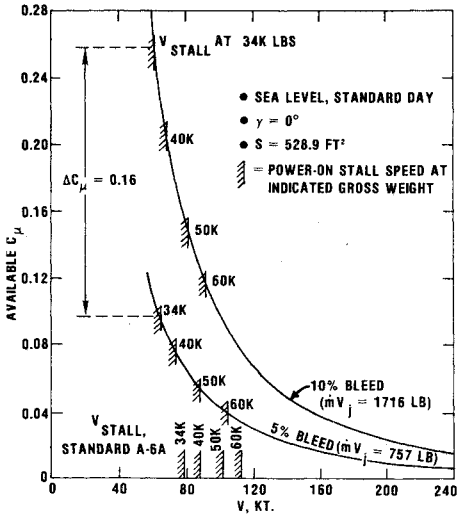

Fig. 15 C_μ available and power-on stall speeds at normal rated thrust.

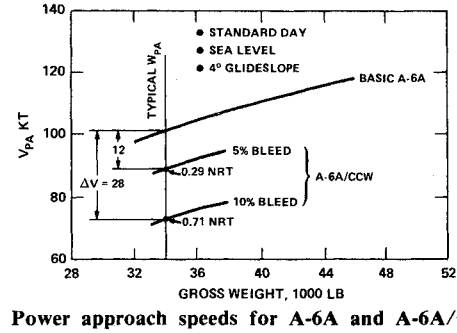

Fig. 16 Power approach speeds for A-6A and A-6A/CCW configuration in equilibrium flight.

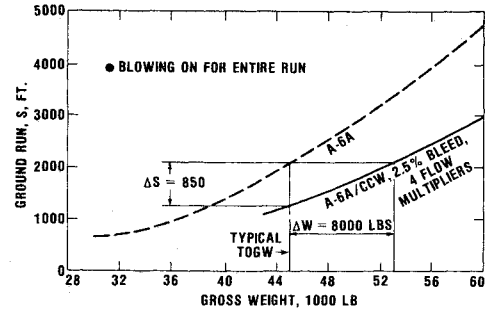

Fig. 17 Takeoff ground runs for A-6A and A-6A/CCW configurations at military thrust.

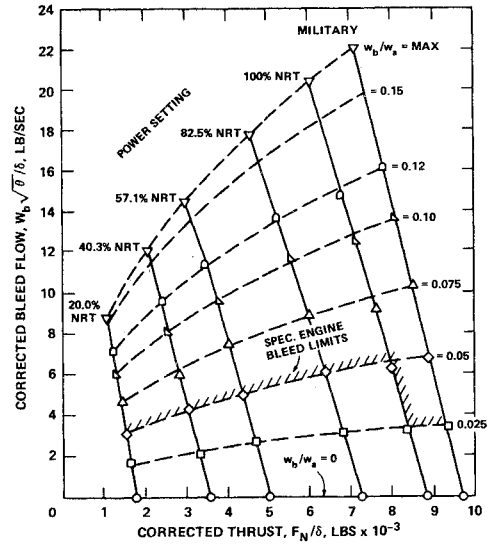

Fig. 18 Uninstalled J-52-P-8A engine performance with bleed.

modification. To investigate application to the flight demonstrator aircraft, the feasibility study contracted to Grumman Aerospace Corporation made use of the wind-tunnel data to predict full-scale power-on STOL performance (Figs. 14-17). Full-scale $C_{L_{max}}$, power-on and off for both the standard A-6 and the CCW, are plotted in Fig. 14 for various aircraft gross weights and two bleed rates. These are trim data for level flight and include an engine vertical thrust component to lift. "Power off" implies aerodynamic $C_{L_{max}}$ with no thrust component but the CCW still powered by engine bleed flow.

For the blown aircraft at constant bleed rate, available $C_{L_{max}}$ varies with weight due to the dependence of C_μ on the velocity and dynamic pressure required for level flight. For the basic A-6A at constant thrust setting, power-on $C_{L_{max}}$ also varies with velocity, because it includes the vertical component of the thrust coefficient (as is also true for CCW). Figure 15 shows these trends in terms of C_μ available at various approach speeds and two bleed rates. The power-on stall speeds (V_{stall}) for varying CCW gross weights are shown in comparison to those of the basic A-6A, where for a 34,000 lb aircraft, a reduction of 18 knots (or 23%) is achieved by the CCW configuration. Power-on approach speeds are shown in Fig. 16, where the approach condition is defined as equilibrium flight at an angle of attack 10 deg less than the stall (Fig. 11), rather than some fixed percentage of $C_{L_{max}}$ or stall speed. Ten percent bleed results in a 28-knot reduction in approach speed. Operation at the higher thrust setting [0.71 normal rated thrust (NRT)] for the 10% bleed case compared to 0.29 NRT at 5% bleed is caused by the requirement to balance the extra-induced drag at the higher available lift, and by the additional thrust loss due to bleed.

Takeoff ground runs for the standard and CCW aircraft at military power are shown in Fig. 17. Although rated engine bleed at this thrust setting is only 2.5%, thrust loss due to bleed is less, and thus aircraft takeoff performance is better than at a higher bleed rate. In one portion of the Grumman study, four auxiliary airflow multipliers were powered by the bleed air, and used to augment direct bleed mass flow; their performance with 5% bleed is seen in Fig. 14 and takeoff performance with 2.5% bleed in Fig. 17. For a typical takeoff gross weight (TOGW) of 45,000 lb, the CCW aircraft ground run was reduced by 850 ft or roughly 40%. The associated reduced takeoff velocity is applicable to carrier catapult launch, where the wind-over-deck or the catapulting force may be reduced accordingly. An alternative to STOL takeoff is to lift off at the conventional velocity and distance and use the increased lift to provide a valuable overload capability. Using the same 2100-ft ground run as the standard A-6 at 45,000 lb, the CCW version can increase its gross weight to 53,000 lb, thereby adding 8000 lb to its payload.

J-52-P-8A Bleed Tests

As much of the preceding performance improvement is dependent upon maximum mass flow which can be bled from the A-6's twin engines, a bleed flow investigation to determine this quantity was undertaken at the Naval Air Propulsion Test Center. Normally, the J-52-P-8A or -8B engine bleed from existing 12th-stage compressor bleed ports is rated at 5% of the total engine airflow at or below NRT, and 2.5% at military power. For the investigation, the three 2.25 in. diam bleed ports were joined to a common manifold, as was an additional 1.25 in. diam port normally reserved for a fuel heater. Bleed air was extracted through a flowmeter at various bleed ratios (W_b/W_a) and power settings, until a maximum bleed rate at each power setting was reached. This maximum was defined as either the point where the bleed ports choked

(and thus no more mass flow could pass for a constant engine power setting and 12th-stage internal pressure) or the maximum exhaust gas temperature limit for the engine. This critical temperature was closely monitored but was never reached during the test. Figure 18 presents the resulting data in the form of corrected bleed mass flow and engine thrust as functions of power setting and bleed ratio. Here, bleed flow W_b is a function of total engine airflow W_a at that bleed setting. At all power settings, choking of the bleed ports allowed a maximum bleed of 16% or more of total engine airflow; this represents a factor of greater than six improvement over the rated bleed at military power, and more than three for all other power settings. Thrust loss due to bleed at power settings of 0.40 NRT and above averaged about 132 lb per lb/s of bleed air. This is favorable in the equilibrium approach, where reduced thrust allows increased glide slopes or reduced velocity, but is somewhat harmful on takeoff due to resulting reduced acceleration. It is for this latter reason that optimized STOL takeoff will probably be made at reduced bleed rates. Nevertheless, with the additional bleed rates verified for this engine, the STOL performance gains of Figs. 15 and 16 appear to underestimate the maximum obtainable with the flight demonstrator aircraft. A 50-hour engine endurance test run at maximum bleed conditions and cyclic power variations verified that no engine damage due to this excess bleed would result over the planned 50-hour flight demonstration program.

Summary and Recommendations

The preceding investigations indicate that the CCW concept is a promising new form of powered high-lift system compatible with the bleed flow from internally mounted turbine engines characteristic of high-performance attack or fighter aircraft. The ability of CCW to more than double the trimmed maximum lift coefficient of the standard A-6 aircraft demonstrates substantial STOL capability of the system. Data provided by the wind-tunnel investigations and the Grumman study have confirmed the feasibility of conducting a full-scale flight test, and have provided a data base for modification of the flight demonstrator aircraft and additional study of its STOL performance.

The wind-tunnel results did indicate that certain improvements to the concept could be made and should be further investigated. Many of the problems encountered in preventing leading-edge separation from both the wing and horizontal stabilizer could be remedied by the use of leading-edge tangential blowing, rather than additional surfaces which would have to be retractable on operational aircraft. On future applications, full-span trailing-edge blowing on the wing would reduce the problems produced by both inboard and outboard vortices at the ends of the blown lifting surface, and a high T-tail removed from wing downwash would simplify trim and control of the STOL aircraft. Differential blowing should be further investigated as a simplified non-deflecting lateral control scheme. Finally, if application to future high-speed aircraft is to be realized, the effects of higher sweep and lower aspect ratios need to be considered.

References

[1] Stone, M. B. and Englar, R. J., "Circulation Control – A Bibliography of NSRDC Research," Naval Ship Research and Development Center Rept. 4108, July 1973.

[2] Englar, R. J., "Investigation into and Application of the High Velocity Circulation Control Wall Jet for High Lift and Drag Generation on STOL Aircraft," AIAA Paper 74-502, Palo Alto, Calif., June 1974.

[3] Englar, R. J., "Subsonic Two-Dimensional Wind Tunnel Investigations of the High Lift Capability of Circulation Control Wing Sections," Naval Ship Research and Development Center Rept. ASED-274, April 1975.

[4] Riebe, J. M., "A Correlation of Two-Dimensional Data on Lift Coefficient Available with Blowing-, Suction-, Slotted-, and Plain-Flap High Lift Devices," NACA RM L55D 29a, Oct. 1955.

[5] Englar, R. J., "Subsonic Wind Tunnel Investigation of the High Lift Capability of a Circulation Control Wing on a 1/5-Scale T-2C Aircraft Model," Naval Ship Research and Development Center Tech. Note AL-299, May 1973.

[6] Englar, R. J., "Circulation Control for High Lift and Drag Generation on STOL Aircraft," *Journal of Aircraft*, Vol. 12, May 1975, pp. 457-463.

[7] Englar, R. J. and Williams, R. M., "Test Techniques for High Lift Two-Dimensional Airfoils with Boundary Layer and Circulation Control for Application to Rotary Wing Aircraft," *Canadian Aeronautics and Space Journal*, Vol. 19, March 1973, pp. 93-108.

[8] Giangrande, G., "Application of the Calderon Flap to a Carrier-Based Jet Aircraft," Grumman Aircraft Engineering Corporation Rept. FSR-427-1, April 1968.

[9] Englar, R. J., Trobaugh, L. A., and Hemmerly, R. A., "Development of the Circulation Control Wing to Provide STOL Potential for High Performance Aircraft," AIAA Paper 77-578, in *A Collection of Technical Papers from the AIAA/NASA Ames V/STOL Conference*, Palo Alto, Calif., June 1977, pp. 74-84.